
PARTITIONED SOLUTION STRATEGIES FOR COUPLED BEM-FEM ACOUSTIC FLUID-STRUCTURE INTERACTION PROBLEMS

*

Luis Rodríguez-Tembleque, José A. González, Antonio Cerrato
Escuela Técnica Superior de Ingeniería
Universidad de Sevilla
Camino de los Descubrimientos s/n, 41092 Sevilla, Spain
{luisroteso, japerez, antoniocerrato}@us.es

2015

ABSTRACT

Abstract: This paper investigates two FEM–BEM coupling formulations for acoustic fluid-structure interaction (FSI) problems, using the Finite Element Method (FEM) to model the structure and the Boundary Element Method (BEM) to represent a linear acoustic fluid. The coupling methods described interconnect fluid and structure using classical or localized Lagrange multipliers, allowing the connection of non-matching interfaces. First coupling technique is the well known mortar method, that uses classical multipliers and is compared with a new formulation of the method of localized Lagrange multipliers (LLM) for FSI applications with non-matching interfaces. The proposed non-overlapping domain decomposition technique uses a classical non-symmetrical acoustic BEM formulation for the fluid, although a symmetric Galerkin BEM formulation could be used as well. A comparison between the localized methodology and the mortar method in highly non conforming interface meshes is presented. Furthermore, the methodology proposes an iterative preconditioned and projected bi-conjugate gradient solver which presents very good scalability properties in the solution of this kind of problems.

Keywords Domain decomposition · FETI · BETI · Fluid–structure interaction · Localized Lagrange multipliers · Mortar

1 Introduction

Reductions in noise emissions have high priority in the design process of vibrating fluid-structure systems. These acoustic fluid-structure interaction (FSI) problems are commonly found in many engineering applications [1], and the numerical simulation of the interaction between the vibrating structure gives fundamental information for optimizing the design of the structure. In some situations one can perform the simulations neglecting the influence of the acoustic field on the vibrating structure. However, this is not acceptable for thin and flexible structures that are easily excited by the acoustic pressure. For these applications the acoustic field has to be fully coupled to the vibrating structure. The finite element method (FEM) have been applied to study this kind of problems, many examples can be found in the book of Ohayon and Soize [2] and Sandberg and Ohayon [3].

The boundary element method (BEM) offers the major advantage over the FEM, that only the boundary of the acoustic domain must be discretized. Moreover, the Sommerfeld radiation condition for exterior domains is inherently fulfilled, so it is especially more appropriate than FEM to study exterior problems (ie. wave propagation in infinite domains). For

**Citation:* Luis Rodríguez-Tembleque, José A. González, Antonio Cerrato, Partitioned solution strategies for coupled BEM–FEM acoustic fluid–structure interaction problems, *Computers & Structures*, Volume 152, 2015, Pages 45-58, ISSN 0045-7949, <https://doi.org/10.1016/j.compstruc.2015.02.018>.

an introduction to the BEM, it is referred to the monograph by Gaul et al. [4]. Coupling boundary element and finite element method in FSI, one can benefit from the advantages of both numerical methodologies: FEM is used to model the structure, and the BEM to model the fluid. The first BEM-FEM coupling algorithm was developed by Everstine and Henderson [5], and later, Chen et al. [6] proposed a variational coupling scheme for Galerkin methods. Further developments and applications of BEM-FEM methods for structure-acoustic field interaction can be found in the works of Gaul and Wenzel [7], Czygan and von Estorff [8], and Langer and Antes [9], and more recently, Fritze et al. [10], Soares [11], He et al. [12] and Soares and Godinho [13].

Based in a mortar scheme, Fischer and Gaul [14] proposed an efficient FEM-BEM coupling in FSI which allows to connect dissimilar meshes, using a to solve coupled acoustical-fluid (BEM) structure (FEM), via classical Lagrange multipliers. The mortar element method was originally introduced by Bernardi et al. [15]. It offers the big advantage, that non-conforming discretizations can be coupled. One obtains great flexibility for meshing the subdomains and an increased efficiency in the case that a coarser mesh is sufficient in one of the subdomains. Formulations, based on classical Lagrange multiplier fields, are quite effective but tend to generate monolithic schemes that do not preserve software modularity. To obtain a partitioned scheme, Park and Felippa [16, 17, 18] proposed a formulation to connect non-matching FEM meshes. Non-matching interfaces are treated by the method of localized Lagrange multipliers (LLM), introducing a discrete surface *frame* interposed between the subdomains to approximate interface displacements. This *frame* is discretized and connected to the BEM or FEM substructures by using LLM collocated at the interface nodes. The application of BEM and FEM coupling in elastostatics using localized Lagrange multipliers has been done by González and Park [19], and the extension to fluid-structure field interaction, by Park et al. [20, 23], Ross et al. [21, 22] and González and Park [24] and González et al. [25].

In the mid-frequency regimes the acoustic fluid-structure problems require fine meshes and, as a result, they generate a large number of degrees of freedom. In this context, domain decomposition methodologies (DDM) have appeared as a powerful numerical tool for solving this large-scale systems. One of the most important strategies is the finite element tearing and interconnecting (FETI) method. The FETI methodology was proposed by Farhat and Roux [26] in the mid-90s, and it is an effective DDM for the parallel solution of finite element problems partitioned into subdomains. The global continuity across the subdomains interfaces is enforced by classical Lagrange multipliers, which leads to a saddle point problem that can be solved iteratively via its dual problem. The dual problem leads to a linear flexibility equations system for the Lagrange multipliers which is solved by a preconditioned conjugate gradient (PCG) algorithm. The success of the FETI method is due to its scalability with respect to the problem size and number of subdomains [27, 28], so the total solution time is approximately constant using a smaller element size by multiplying proportionately the number of processors. The numerical effort needed to solve the flexibility system iteratively using a PCG algorithm is controlled by the condition number of the system. Farhat et al. [28, 29, 30] and Mandel and Tezaur [31] estimated the condition number of the system for the FETI method as a function of the number of element per subdomain: $\mathcal{O}((1 + \log(L/h))^2)$. Here, L and h denote the average size of the subdomains and finite elements, respectively. Note that condition number is bounded independently of the number of subdomains, so it is a necessary condition to achieve numerical scalability. For some further development of the FETI methodology (FETI-DP), the reader can turn to [32, 33], and its application to acoustics FSI problems, to Farhat et al. [34, 35] and Li et al. [36].

The Boundary Element Tearing and Interconnecting (BETI) method came up as a direct extension of the FETI to the BEM. The BETI method was recently introduced by Langer and Steinbach [37] as a counter part of the FETI methods. This methodology extends the tearing and interconnecting technique to symmetric Galerkin boundary element method (SGBEM) [38, 39] in order to obtain symmetric system matrices and, therefore, the use of FETI PCG solver becomes feasible. The SGBEM is used to construct the *Steklov-Poincaré* operators instead of the finite element based Schur complements, so the advantageous properties of FETI methods remain valid for BETI methods as well. It can be demonstrated numerically [37, 40] that, using a preconditioner with appropriated scaling matrices, the condition number of the preconditioned BETI system is $\mathcal{O}((1 + \log(L/h))^2)$, providing the same scalability characteristics than the FETI method. This BETI methodology has been successfully applied to different kind of problems (i.e. Bouchala et al. [41] proposed a BETI scheme for contact problems), but it requires the implementation of SGBEM, what is not straightforward. If it is replaced by a non-symmetrical BEM formulation to approximate the *Steklov-Poincaré* operators of the floating substructures, the flexibility equations become non-symmetric and different solution strategies should be considered.

This work presents a non-symmetric FE-BETI formulation to solve vibro-acoustic FSI problems based on [42, 43, 44]. The resulting non-symmetrical flexibility system is solved by a new iterative solution procedure based in a Bi-Conjugate Gradient Stabilized (Bi-CGSTAB) algorithm. The formulation is presented together with some benchmark examples that allow to compare the mortar and LLM schemes for non-conforming approximations, and to check convergence and accuracy of the non-symmetric FE-BETI algorithm as well as scalability properties.

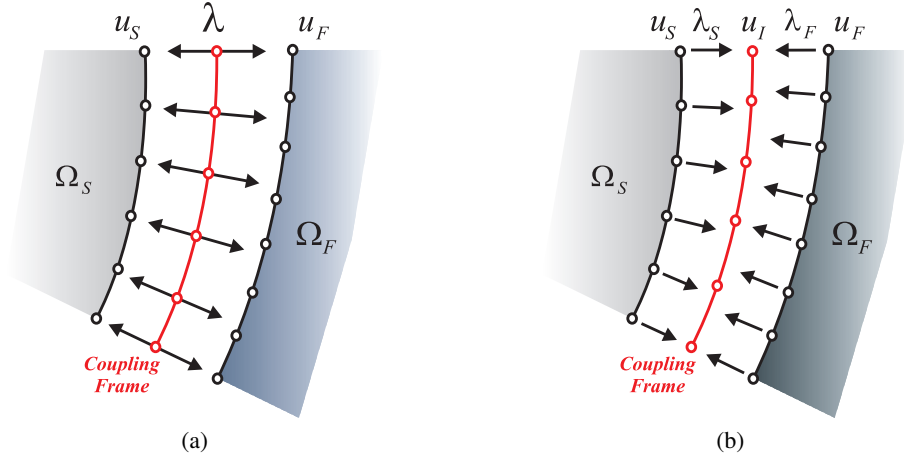


Figure 1: Differences in the description of mortar (a) and localized (b) interfaces. Classical multipliers are used in (a) with a direct connection of the interfaces. In (b), an independent discretization of the interface is introduced and connected to the solid and fluid boundaries using localized Lagrange multipliers.

The paper is organised as follows. After the introduction, an acoustics FSI partitioned formulation is developed. In Section 3, special attention is paid to the choice of the coupling strategy: mortar or LLM. The projected Bi-Conjugate Gradient Stabilized is presented in Section 4, and scalability and convergence issues are studied on different examples in Section 5. Finally, the paper concludes with the summary and resulting conclusions.

2 Acoustics FSI partitioned formulation

A FEM structure and a BEM fluid domain are considered, so the total virtual work of the system δW_T can be expressed as the addition of the virtual work done by the FEM structure domain δW_S , the BEM fluid domain δW_F and the interface coupling contribution δW_C ,

$$\delta W_T = \delta W_S + \delta W_F + \delta W_C \quad (1)$$

2.1 Structural domain

The virtual work of a flexible structure, δW_S , is described by the principle of virtual work for a continuum body with domain Ω_S and surface Γ_S that, assuming small displacements, can be written:

$$\begin{aligned} \delta W_S = & \int_{\Omega_S} \sigma_{Sij} \delta u_{Si,j} d\Omega - \int_{\Omega_S} (\rho_S \omega^2 u_{Si} + b_{Si}) \delta u_{Si} d\Omega \\ & - \int_{\Gamma_S} t_{Si} \delta u_{Si} d\Gamma \end{aligned} \quad (2)$$

where u_{Si} is the i -th component of the structural displacement vector, a vector with the same number of components than the dimension of the space; σ_{Sij} is the Cauchy stresses tensor, t_{Si} the applied surface tractions and b_{Si} the body forces. Finally, ω and ρ_S are the angular frequency of the harmonic oscillations and the density of the structural material, respectively.

Next, the structure is discretized using the classical FEM approximation, where the assembly of element contributions by the direct stiffness method leads to the semidiscrete equation of motion:

$$\delta W_S = \delta \mathbf{u}_S^T \{ (\mathbf{K}_S - \omega^2 \mathbf{M}_S) \mathbf{u}_S - \mathbf{f}_S \} \quad (3)$$

where \mathbf{K}_S is the stiffness matrix, \mathbf{M}_S is the mass matrix, \mathbf{u}_S is the vector of nodal displacements and \mathbf{f}_S are the applied nodal forces. Equation (3) can be written in a more compact form:

$$\delta W_S = \delta \mathbf{u}_S^T \{ \bar{\mathbf{K}}_S \mathbf{u}_S - \mathbf{f}_S \} \quad (4)$$

defining the dynamic stiffness matrix as $\bar{\mathbf{K}}_S = \mathbf{K}_S - \omega^2 \mathbf{M}_S$.

2.2 Acoustic-fluid domain

The governing equation for the linear acoustic fluid with domain Ω_F is the Helmholtz equation:

$$\nabla^2 p_F + k_F^2 p_F = 0 \quad (5)$$

In this equation, ∇^2 is the Laplacian, p_F is the acoustic fluid pressure, $k_F = \omega/c_F$ the wave number, c_F the speed of sound in the fluid and ω the frequency.

On the fluid boundary $\Gamma_F = \Gamma_{Fu} \cup \Gamma_{Fr}$, two types of boundary condition are considered:

- Neumann boundary condition:

$$\frac{\partial p_F}{\partial n} = \rho_F \omega^2 u_{Fn} \quad \text{on } \Gamma_{Fu} \quad (6)$$

- Rigid boundary:

$$\frac{\partial p_F}{\partial n} = 0 \quad \text{on } \Gamma_{Fr} \quad (7)$$

where n denotes the unit normal on the surface, ρ_F is the fluid density and u_{Fn} represents the amplitude of the normal displacement on the boundary.

The BEM formulation for a linear acoustic medium is well known and can be found in many classical texts [45] and it is based on the transformation of Helmholtz equation (5) into a boundary integral equation. To do so, Helmholtz equation is written in a weak form considering a weighted residual approach using the Green's function $G(\mathbf{x}, \mathbf{y})$ as the weighting function, being \mathbf{x} the collocation point and \mathbf{y} the source point. The expression of the Green's function depends on the dimension of the space, with:

$$G(\mathbf{x}, \mathbf{y}) = \frac{i}{4} H_0^{(1)}(k_F |\mathbf{x} - \mathbf{y}|) \quad (8)$$

for two dimensions, where $H_0^{(1)}$ is the Hankel function of the first kind and i is the imaginary unit.

Applying Green's second theorem to the weighted residual and locating the collocation point on the boundary, the resulting boundary integral equation is:

$$\begin{aligned} C(\mathbf{x})p_F(\mathbf{x}) + \int_{\Gamma_F} p_F(\mathbf{y}) \frac{\partial G(\mathbf{x}, \mathbf{y})}{\partial n} d\Gamma = \\ \int_{\Gamma_F} G(\mathbf{x}, \mathbf{y}) \frac{\partial p_F(\mathbf{y})}{\partial n} d\Gamma \end{aligned} \quad (9)$$

where $C(\mathbf{x})$ is a coefficient that depends on the position of point \mathbf{x} : $C(\mathbf{x}) = 1$ for an internal point, $C(\mathbf{x}) = \frac{1}{2}$ for \mathbf{x} on a smooth boundary Γ_F , and $C(\mathbf{x}) = 0$ for an external point.

Taking into account the Neumann boundary condition (6), equation (9) can be rewritten as:

$$\begin{aligned} C(\mathbf{x})p_F(\mathbf{x}) + \int_{\Gamma_F} p_F(\mathbf{y}) \frac{\partial G(\mathbf{x}, \mathbf{y})}{\partial n} d\Gamma = \\ \rho_F \omega^2 \int_{\Gamma_{Fu}} G(\mathbf{x}, \mathbf{y}) u_{Fn}(\mathbf{x}) d\Gamma \end{aligned} \quad (10)$$

Next, the BIE is discretized dividing the fluid boundary Γ_F into n_e linear elements of surface Γ_e . Pressure and displacement fields are approximated on each element Γ_e by using linear shape functions:

$$p_F = \sum_{i=1}^m N_i p_{Fi} = \mathbf{N} \mathbf{p}_F \quad (11)$$

$$u_{Fn} = \sum_{i=1}^m N_i u_{Fni} = \mathbf{N} \mathbf{u}_F \quad (12)$$

where p_{Fi} and u_{Fni} are the nodal values of acoustic pressure and fluid normal displacement at node i , and \mathbf{N} is the shape function approximation matrix. A discrete boundary integral equation is then obtained substituting equation (11)

into equation (10) and considering that the point \mathbf{x} is collocated on a boundary node:

$$\begin{aligned} C_i \delta_{ij} p_{Fj} + \sum_{e=1}^{n_e} \int_{\Gamma_e} \frac{\partial G(\mathbf{x}, \mathbf{y})}{\partial n} N_j p_{Fj} d\Gamma_e = \\ \rho_F \omega^2 \sum_{e=1}^{n_e} \int_{\Gamma_e} G(\mathbf{x}, \mathbf{y}) N_j u_{Fnj} d\Gamma_e \end{aligned} \quad (13)$$

being δ_{ij} is the Kronecker δ -function. Equation (13) can be written in matrix form as:

$$\mathbf{H} \mathbf{p}_F = \mathbf{G} \mathbf{u}_F \quad (14)$$

with the following definition for the matrix components:

$$H_{ij} = C_i \delta_{ij} + \sum_{e=1}^{n_e} \int_{\Gamma_e} \frac{\partial G(\mathbf{x}, \mathbf{y})}{\partial n} N_j d\Gamma_e \quad (15)$$

$$G_{ij} = \rho_F \omega^2 \sum_{e=1}^{n_e} \int_{\Gamma_e} G(\mathbf{x}, \mathbf{y}) N_j d\Gamma_e \quad (16)$$

The virtual work of a BEM fluid subdomain can then be computed using a weak statement for dynamic equilibrium reduced to the boundary. This is done with Clapeyron equation [46, 19] that is expressed in the following form:

$$\delta W_F = \int_{\Gamma_F} (p_F - t_F) \delta u_{Fn} d\Gamma \quad (17)$$

defining the external normal tractions imposed on the boundary as t_F and where the fluid pressure p_F satisfies equation (9).

Discretizing equation (17) using the same BEM mesh utilized for the fluid, a discrete approximation of the virtual work is obtained:

$$\begin{aligned} \delta W_F &= \delta \mathbf{u}_F^T \left[\int_{\Gamma_F} \mathbf{N}^T \mathbf{N} d\Gamma \right] \{ \mathbf{p}_F - \mathbf{t}_F \} \\ &= \delta \mathbf{u}_F^T \mathbf{M} \{ \mathbf{p}_F - \mathbf{t}_F \} \end{aligned} \quad (18)$$

with a lumping matrix

$$\mathbf{M} = \int_{\Gamma_F} \mathbf{N}^T \mathbf{N} d\Gamma \quad (19)$$

that transforms distributed tractions into equivalent nodal forces.

Substituting the discrete fluid pressures \mathbf{p}_F coming from the BE equation (14) into the variational form (18), a final expression for the discrete variation is obtained:

$$\delta W_F = \delta \mathbf{u}_F^T \mathbf{M} \{ \rho_F \omega^2 \mathbf{H}^{-1} \mathbf{G} \mathbf{u}_F - \mathbf{t}_F \} \quad (20)$$

Note that this variational statement, obtained from a boundary integral formulation, in general does not derive from an energy functional and will be non-symmetric.

By comparison with equation (4), we conclude that the equations for the fluid and the structure can be written using the same expression:

$$\delta W_F = \delta \mathbf{u}_F^T \{ \bar{\mathbf{K}}_F \mathbf{u}_F - \mathbf{f}_F \} \quad (21)$$

simply by defining an equivalent dynamic stiffness matrix for the fluid $\bar{\mathbf{K}}_F = \rho_F \omega^2 \mathbf{M} \mathbf{H}^{-1} \mathbf{G}$ and the vector of given external forces as $\mathbf{f}_F = \mathbf{M} \mathbf{t}_F$.

3 Coupling strategies

Two different strategies are investigated in this Section for the connection of the fluid and the structure: *Mortar* method and the method of *localized Lagrange multipliers*. A general formulation is derived first for both methodologies and then they are compared using a classical FSI example from [47].

3.1 Mortar method

We consider two coupled subdomains, Ω_S and Ω_F , sharing a common interface Γ_C . In Mortar methods, the work associated to the tying interface will enforce the coupling condition in a weak sense through the following expression:

$$W_C = \int_{\Gamma_C} \lambda(u_{Sn} - u_{Fn}) d\Gamma \quad (22)$$

where λ is the Lagrange Multiplier traction field over the coupling interface Γ_C , and u_{Sn} and u_{Fn} are the structure and fluid normal displacement fields over Γ_C . The variation of this form leads to:

$$\begin{aligned} \delta W_C &= \int_{\Gamma_C} \delta\lambda(u_{Sn} - u_{Fn}) d\Gamma + \int_{\Gamma_C} \delta u_{Sn} \lambda d\Gamma \\ &\quad - \int_{\Gamma_C} \delta u_{Fn} \lambda d\Gamma \end{aligned} \quad (23)$$

The interface normal tractions λ and the boundary normal displacements u_n of each domain (S, F) are interpolated on the boundary as follows:

$$\lambda = \sum_{i=1}^{n_I} \hat{N}_i \lambda_i \quad (24)$$

$$u_{Sn} = \sum_{i=1}^{n_S} N_{Si} u_{Sni}, \quad u_{Fn} = \sum_{i=1}^{n_F} N_{Fi} u_{Fni} \quad (25)$$

where the shape functions (N_{Si}, N_{Fi}) are defined independently for the solid and the fluid side, (u_{Sni}, u_{Fni}) are the structure and fluid normal nodal displacements and (n_I, n_F, n_S) are the number of interface, fluid and structure boundary nodes.

Lagrange multipliers are approximated using linear shape functions \hat{N}_i with the support of the discretisation on the solid non-mortar side, same approximation than in [15]. When Dirichlet boundary conditions exist on the boundary of Γ_C , the shape functions \hat{N}_i have to be modified to avoid over-constrained conditions at those restricted edges [48], as represented in Figure 2.

Substituting approximations (24) and (25) in the mortar coupling equation (23), the boundary integrals can be approximated:

$$\begin{aligned} \int_{\Gamma_C} \delta u_{Sn} \lambda d\Gamma &= \\ \sum_{e=1}^{n_e} \sum_{i=1}^{n_F} \sum_{j=1}^{n_S} \delta u_{Sni} \left[\int_{\Gamma_e} N_{Si} \hat{N}_j d\Gamma \right] \lambda_j \end{aligned} \quad (26)$$

$$\begin{aligned} \int_{\Gamma_C} \delta u_{Fn} \lambda d\Gamma &= \\ \sum_{e=1}^{n_e} \sum_{i=1}^{n_F} \sum_{j=1}^{n_S} \delta u_{Fni} \left[\int_{\Gamma_e} N_{Fi} \hat{N}_j d\Gamma \right] \lambda_j \end{aligned} \quad (27)$$

where n_e is the number of elements on the non-mortar side and Γ_e is the element e boundary (see Figure 3). The boundary integrals of equations (26) and (27) are assembled into matrices \mathbf{A}_S and \mathbf{A}_F , so equation (23) can be written in matrix form as follows:

$$\begin{aligned} \delta W_C &= \delta\boldsymbol{\lambda}^T (\mathbf{A}_S^T \mathbf{u}_{Sn} + \mathbf{A}_F^T \mathbf{u}_{Fn}) \\ &\quad + (\delta\mathbf{u}_{Sn})^T \mathbf{A}_S \boldsymbol{\lambda} + (\delta\mathbf{u}_{Fn})^T \mathbf{A}_F \boldsymbol{\lambda} \end{aligned} \quad (28)$$

being $\boldsymbol{\lambda}$, \mathbf{u}_{Sn} and \mathbf{u}_{Fn} the vectors of nodal tractions, and nodal structure and fluid interface normal displacements.

Normal displacement vectors on the boundary, \mathbf{u}_{Sn} and \mathbf{u}_{Fn} , can be obtained from the global vectors of structure and fluid displacements:

$$\mathbf{u}_{Sn} = \mathbf{B}_S^T \mathbf{u}_S, \quad \mathbf{u}_{Fn} = \mathbf{B}_F^T \mathbf{u}_F \quad (29)$$

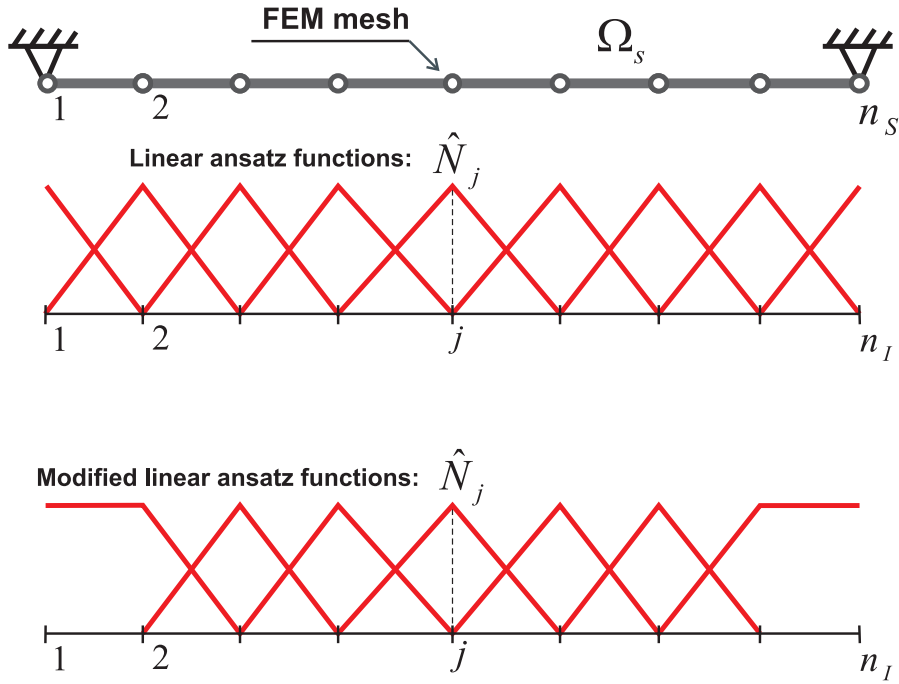


Figure 2: Modified linear ansatz functions used with Mortar method in the presence of Dirichlet boundary conditions for the approximation of interface Lagrange multipliers.

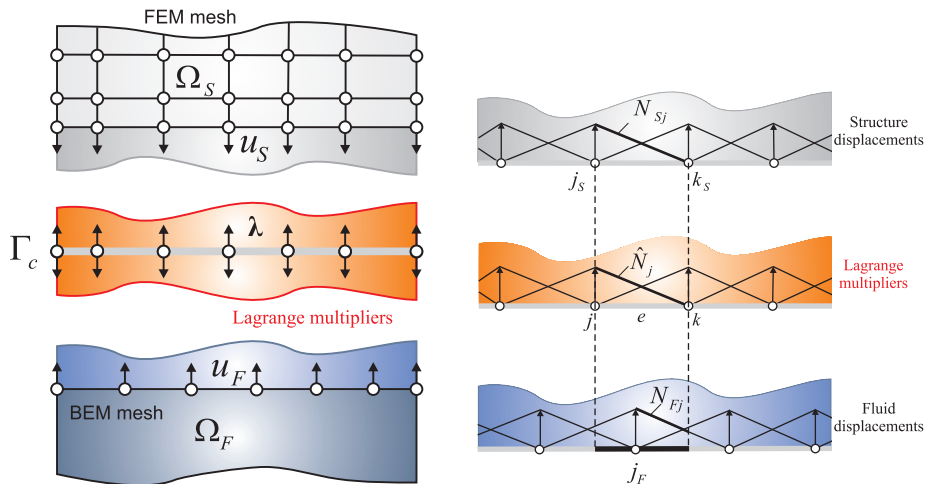


Figure 3: Coupling with the Mortar method fluid and solid interfaces. Approximation spaces for boundary displacements and multipliers.

where \mathbf{B}_S and \mathbf{B}_F are boolean matrices. Substituting (29) into (28) and defining the coupling matrices:

$$\mathbf{C}_S = \mathbf{B}_S \mathbf{A}_S, \quad \mathbf{C}_F = \mathbf{B}_F \mathbf{A}_F \quad (30)$$

we arrive to the following expression for the virtual work of the interface:

$$\delta W_C = \delta \boldsymbol{\lambda}^\top (\mathbf{C}_S^\top \mathbf{u}_S + \mathbf{C}_F^\top \mathbf{u}_F) + \delta \mathbf{u}_S^\top \mathbf{C}_S \boldsymbol{\lambda} + \delta \mathbf{u}_F^\top \mathbf{C}_F \boldsymbol{\lambda} \quad (31)$$

Total virtual work of the system δW_T is then derived from (4), (21) and (31) as:

$$\begin{aligned} \delta W_T = & \delta \mathbf{u}_S^\top \{ \bar{\mathbf{K}}_S \mathbf{u}_S + \mathbf{C}_S \boldsymbol{\lambda} - \mathbf{f}_S \} + \\ & \delta \mathbf{u}_F^\top \{ \bar{\mathbf{K}}_F \mathbf{u}_F + \mathbf{C}_F \boldsymbol{\lambda} - \mathbf{f}_F \} + \delta \boldsymbol{\lambda}^\top \{ \mathbf{C}_S^\top \mathbf{u}_S + \mathbf{C}_F^\top \mathbf{u}_F \} \end{aligned} \quad (32)$$

and from the stationary-point condition of this virtual work, the following partitioned FSI equation set is obtained:

$$\begin{bmatrix} \bar{\mathbf{K}}_S & \mathbf{0} & \mathbf{C}_S \\ \mathbf{0} & \bar{\mathbf{K}}_F & \mathbf{C}_F \\ \mathbf{C}_S^\top & \mathbf{C}_F^\top & \mathbf{0} \end{bmatrix} \begin{bmatrix} \mathbf{u}_S \\ \mathbf{u}_F \\ \boldsymbol{\lambda} \end{bmatrix} = \begin{bmatrix} \mathbf{f}_S \\ \mathbf{f}_F \\ \mathbf{0} \end{bmatrix} \quad (33)$$

In general, for $p = 1 \dots n_p$ fluid and structure partitions, equation (33) can be expressed in condensed form as:

$$\begin{bmatrix} \mathbf{K} & \mathbf{C} \\ \mathbf{C}^\top & \mathbf{0} \end{bmatrix} \begin{bmatrix} \mathbf{u} \\ \boldsymbol{\lambda} \end{bmatrix} = \begin{bmatrix} \mathbf{f} \\ \mathbf{0} \end{bmatrix} \quad (34)$$

by simply defining the block-matrices:

$$\mathbf{K} = \text{diag} \left[\mathbf{K}_\star^{(1)} \dots \mathbf{K}_\star^{(n_p)} \right], \quad \mathbf{C} = \begin{bmatrix} \mathbf{C}_\star^{(1)} \\ \vdots \\ \mathbf{C}_\star^{(n_p)} \end{bmatrix} \quad (35)$$

and block-vectors:

$$\mathbf{u} = \begin{Bmatrix} \mathbf{u}_\star^{(1)} \\ \vdots \\ \mathbf{u}_\star^{(n_p)} \end{Bmatrix}, \quad \mathbf{f} = \begin{Bmatrix} \mathbf{f}_\star^{(1)} \\ \vdots \\ \mathbf{f}_\star^{(n_p)} \end{Bmatrix} \quad (36)$$

with subscript $\star = S, F$ indicating the type of model associated to substructure p , i.e., (S) for solid modeled using FEM or (F) for acoustic fluid using BEM.

After this reorganization and eliminating the displacements \mathbf{u} from the first row of (34) using the relation:

$$\mathbf{u} = \mathbf{K}^{-1} (\mathbf{f} - \mathbf{C} \boldsymbol{\lambda}) \quad (37)$$

a compact non-symmetrical flexibility system is obtained:

$$\mathbf{F}_{bb} \boldsymbol{\lambda} = \mathbf{b} \quad (38)$$

being $\mathbf{F}_{bb} = \mathbf{C}^\top \mathbf{K}^{-1} \mathbf{C}$ a boundary flexibility matrix and $\mathbf{b} = \mathbf{C}^\top \mathbf{K}^{-1} \mathbf{f}$ the free term.

3.2 Localized Lagrange multipliers method

The virtual work for the interface frame δW_C can be also evaluated applying the variationally-based formulation proposed by Park and Felippa [16, 17] and González et al. [19]. The virtual work of the total system δW_T consists of contributions from the FE structure and BE fluid, δW_S and δW_F , plus the interface frame δW_C . This formulation enforces the kinematical positioning of the frame in a weak sense with the following expression:

$$W_C = \int_{\Gamma_C} \{ \lambda_S (u_{S_n} - u_{I_n}) + \{ \lambda_F (u_{F_n} - u_{I_n}) \} d\Gamma \quad (39)$$

where both integrals are extended to the boundary interface Γ_C . The localized Lagrange multipliers and the displacements of the structure interface are represented by (λ_S, u_{S_n}) , and the fluid localized Lagrange multipliers and displacements by (λ_F, u_{F_n}) . Finally, the frame displacements are represented by u_{I_n} .

Equation (39) can be written in matrix form as:

$$\delta W_C = \delta \{ \boldsymbol{\lambda}_S^\top (\mathbf{B}_S^\top \mathbf{u}_S - \mathbf{L}_S \mathbf{u}_I) \} + \delta \{ \boldsymbol{\lambda}_F^\top (\mathbf{B}_F^\top \mathbf{u}_F - \mathbf{L}_F \mathbf{u}_I) \} \quad (40)$$

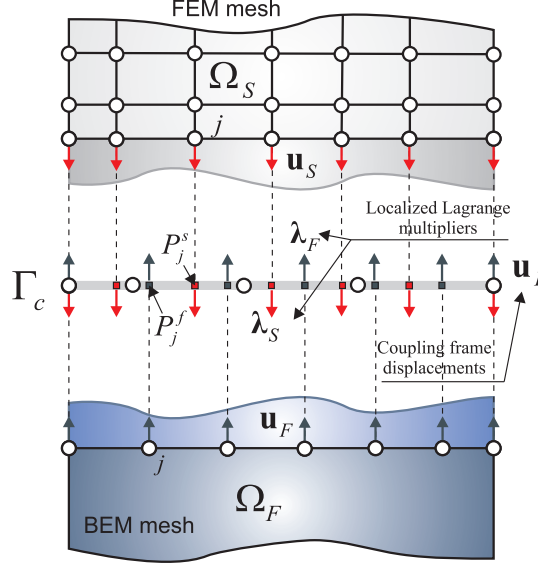


Figure 4: FSI BEM-FEM system with intercalated frame and localized Lagrange multipliers.

using two linear operators, \mathbf{B}_S to extract the structural boundary displacements projected into the normal direction and \mathbf{B}_F to extract the fluid boundary displacements. \mathbf{L}_S and \mathbf{L}_F [18, 19] are matrices whose terms are obtained by evaluating the frame shape functions at the interface nodal position of the structure and fluid P_j^s and P_j^f (see Figure 4). The total virtual work of the coupled BEM-FEM-Frame system can finally be expressed as:

$$\begin{aligned} \delta W_T = & \delta \mathbf{u}_S^T \{ \bar{\mathbf{K}}_S \mathbf{u}_S + \mathbf{B}_S \boldsymbol{\lambda}_S - \mathbf{f}_S \} + \\ & \delta \mathbf{u}_F^T \{ \bar{\mathbf{K}}_F \mathbf{u}_F + \mathbf{B}_F \boldsymbol{\lambda}_F - \mathbf{f}_F \} + \delta \boldsymbol{\lambda}_S^T \{ \mathbf{B}_S^T \mathbf{u}_S - \mathbf{L}_S \mathbf{u}_I \} \\ & + \delta \boldsymbol{\lambda}_F^T \{ \mathbf{B}_F^T \mathbf{u}_F - \mathbf{L}_F \mathbf{u}_I \} + \delta \mathbf{u}_I^T \{ \mathbf{L}_S^T \boldsymbol{\lambda}_S + \mathbf{L}_F^T \boldsymbol{\lambda}_F \} \end{aligned} \quad (41)$$

The stationarity condition of this variational form provides the equations of motion, defined by the following system:

$$\begin{bmatrix} \bar{\mathbf{K}}_S & \mathbf{0} & \mathbf{B}_S & \mathbf{0} & \mathbf{0} \\ \mathbf{0} & \bar{\mathbf{K}}_F & \mathbf{0} & \mathbf{B}_F & \mathbf{0} \\ \mathbf{B}_S^T & \mathbf{0} & \mathbf{0} & \mathbf{0} & \mathbf{L}_S \\ \mathbf{0} & \mathbf{B}_F^T & \mathbf{0} & \mathbf{0} & \mathbf{L}_F \\ \mathbf{0} & \mathbf{0} & \mathbf{L}_S^T & \mathbf{L}_F^T & \mathbf{0} \end{bmatrix} \begin{bmatrix} \mathbf{u}_S \\ \mathbf{u}_F \\ \boldsymbol{\lambda}_S \\ \boldsymbol{\lambda}_F \\ \mathbf{u}_I \end{bmatrix} = \begin{bmatrix} \mathbf{f}_S \\ \mathbf{f}_F \\ \mathbf{0} \\ \mathbf{0} \\ \mathbf{0} \end{bmatrix} \quad (42)$$

In general, if we have n_p different fluid and structure partitions, equation (42) can be written in a more compact form:

$$\begin{bmatrix} \mathbf{K} & \mathbf{B} & \mathbf{0} \\ \mathbf{B}^T & \mathbf{0} & \mathbf{L} \\ \mathbf{0} & \mathbf{L}^T & \mathbf{0} \end{bmatrix} \begin{bmatrix} \mathbf{u} \\ \boldsymbol{\lambda} \\ \mathbf{u}_I \end{bmatrix} = \begin{bmatrix} \mathbf{f} \\ \mathbf{0} \\ \mathbf{0} \end{bmatrix} \quad (43)$$

by defining the following block matrices and vectors:

$$\mathbf{B} = \mathbf{diag} \left[\mathbf{B}_\star^{(1)} \dots \mathbf{B}_\star^{(n_p)} \right] \quad (44)$$

$$\mathbf{L} = \begin{bmatrix} \mathbf{L}_\star^{(1)} \\ \vdots \\ \mathbf{L}_\star^{(n_p)} \end{bmatrix}, \quad \boldsymbol{\lambda} = \begin{Bmatrix} \boldsymbol{\lambda}_\star^{(1)} \\ \vdots \\ \boldsymbol{\lambda}_\star^{(n_p)} \end{Bmatrix} \quad (45)$$

with $\star = S, F$ depending on the physics associated to substructure p , i.e., (S) for a structure modeled using the FEM or (F) for an acoustic fluid approximated with the BEM.

Finally, we are interested in solving the problem first for the interface. This can be done obtaining the subdomain displacements from the first row of (43):

$$\mathbf{u} = \mathbf{K}^{-1}(\mathbf{f} - \mathbf{B}\boldsymbol{\lambda}) \quad (46)$$

and substituting into the second row to obtain the following flexibility system:

$$\begin{bmatrix} \mathbf{F}_{bb} & \mathbf{L} \\ \mathbf{L}^\top & \mathbf{0} \end{bmatrix} \begin{bmatrix} \boldsymbol{\lambda} \\ \mathbf{u}_I \end{bmatrix} = \begin{bmatrix} \mathbf{b} \\ \mathbf{0} \end{bmatrix} \quad (47)$$

with $\mathbf{F}_{bb} = \mathbf{B}^\top \mathbf{K}^{-1} \mathbf{B}$ and $\mathbf{b} = \mathbf{B}^\top \mathbf{K}^{-1} \mathbf{f}$.

3.3 Test: Mortar-MLL comparisson

The coupling possibilities of Mortar and LLM methodologies are studied and compared by solving the following test problem taken from [47]: a two dimensional $L \times H$ cavity ($L = 10 \text{ m}$ and $H = 4 \text{ m}$) with one flexible side (see Figure 5). The flexible wall is a beam that is simply supported on both edges of the cavity and is modeled using Euler-Bernoulli beam elements. The properties of this structural domain are: Young module $E = 2.1 \times 10^{11} \text{ Pa}$, section inertia $I = 1.59 \times 10^{-4} \text{ m}^4$, cross section area $A = 0.02 \text{ m}^2$ and a mass per unit length $m_s = 50 \text{ kg/m}$. The remaining three sides of the cavity are reverberant walls where homogeneous Neumann boundary conditions are applied ($v_n = 0$). The fluid is water with $c_F = 1500 \text{ m/s}$ and $\rho_F = 1000 \text{ kg/m}^3$. The sketch of this problem is presented in Figure 5(a) where a harmonic bending moment $M_{exc} = M_o e^{i\omega t}$ is applied in one edge. In Figure 5(b) an scheme of the meshes and the coupled BEM-FEM subdomains using LLM is presented.

Figure 6 shows the beam rotation at $x = L$ as a function of the excitation frequency. The results coincide with the natural frequencies obtained by Sandberg et al. in [47]. In Figure 7 it can be observed the flexible wall deflection and fluid pressure due to excitations of 5 Hz and 80 Hz, for matching Figure 7(a) and non-matching Figure 7(b) meshes.

The coupling interface displacements of the structure and the fluid obtained using matching meshes with the mortar method and the LLM method are presented in Figure 8, for an harmonic excitations of 5 Hz. As it is observed in Figure 8(a-b) and Figure 8(c-d) both methodologies present the same coupling behavior using matching meshes at the interfaces. However, Figure 9 presents the coupling interface displacements computed using nonmatching meshes with the mortar and the LLM method. It can be observed in Figure 9(a-b) that we obtain inaccuracies in the form of wiggles on the fluid displacements using the mortar method. The appearance of these artifacts in the mortar solution is attributed to the use of different displacement interpolations for the fluid (linear shape functions) and the structure (Hermite polynomials). One main characteristic of mortar methods is that the condition of pointwise continuity across the interface is replaced by a weak form and this standard primal approach is suboptimal when mixed finite element discretizations are used [48]. For this reason, LLM method is going to be used in the nsBE-FETI methodology.

4 Iterative solution strategy for the interface problem

The solution strategy presented to solve the flexibility system obtained for the FSI localized Lagrange multipliers formulation (47) uses a projection of the interface solution vector in the form:

$$\boldsymbol{\lambda} = \mathcal{P}\boldsymbol{\lambda}_d \quad (48)$$

with the symmetric projector defined as:

$$\mathcal{P} = \mathbf{I} - \mathbf{L}(\mathbf{L}^\top \mathbf{L})^{-1} \mathbf{L}^\top \quad (49)$$

satisfying the condition: $\mathcal{P}\mathbf{L} = \mathbf{0}$.

Substitution of this decomposition into the flexibility formulation of the interface problem (47) yields the following equation:

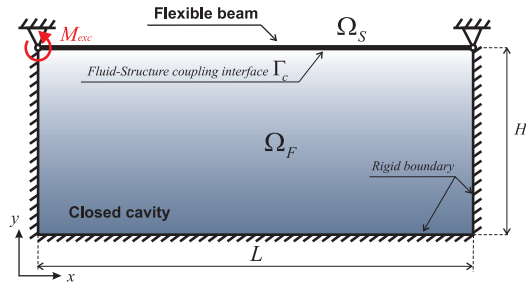
$$\mathcal{P}\mathbf{F}_{bb}\mathcal{P}\boldsymbol{\lambda}_d = \mathcal{P}\mathbf{b} \quad (50)$$

So the projected residual is then finally given by:

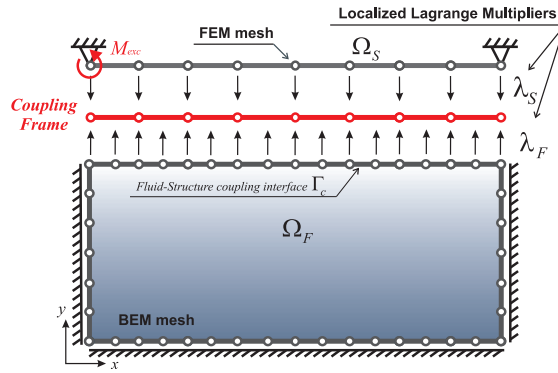
$$\mathbf{r} = \mathcal{P}(\mathbf{b} - \mathbf{F}_{bb}\mathcal{P}\boldsymbol{\lambda}_d) \quad (51)$$

equation that is solved for $\mathcal{P}\boldsymbol{\lambda}_d$.

Because the non-symmetrical BEM-FEM interface problem is usually very large in practical applications, Krylov's iterative schemes for non-symmetrical systems like Bi-CGSTAB and GMRES are preferred for the minimization of residual (51). The authors introduced in [44] a projected Bi-CGSTAB algorithm for non-symmetrical BEM problems in statics. This projected Bi-CGSTAB iterative scheme is generalized to dynamics in Table 1 for the proposed nsBE-FETI formulation.



(a)



(b)

Figure 5: Acoustic cavity with a flexible wall and harmonic excitation. Problem definition (a) and BEM-FEM subdomains coupled using LLM (b).

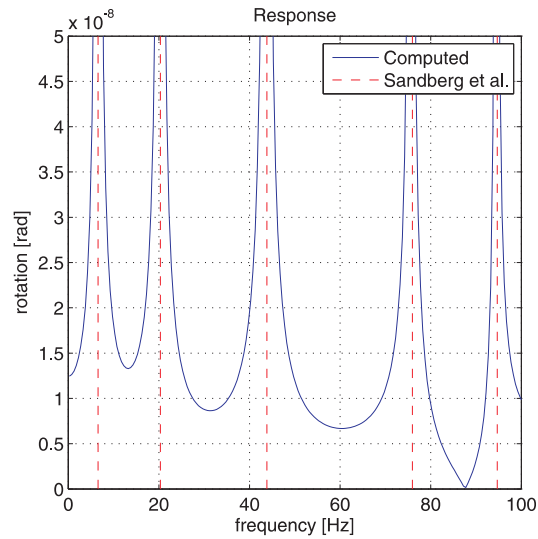


Figure 6: Transfer function of the cavity problem for the beam rotation at $x = L$. Natural frequencies computed by Sandberg et al. [47] using a FEM-FEM coupling method.

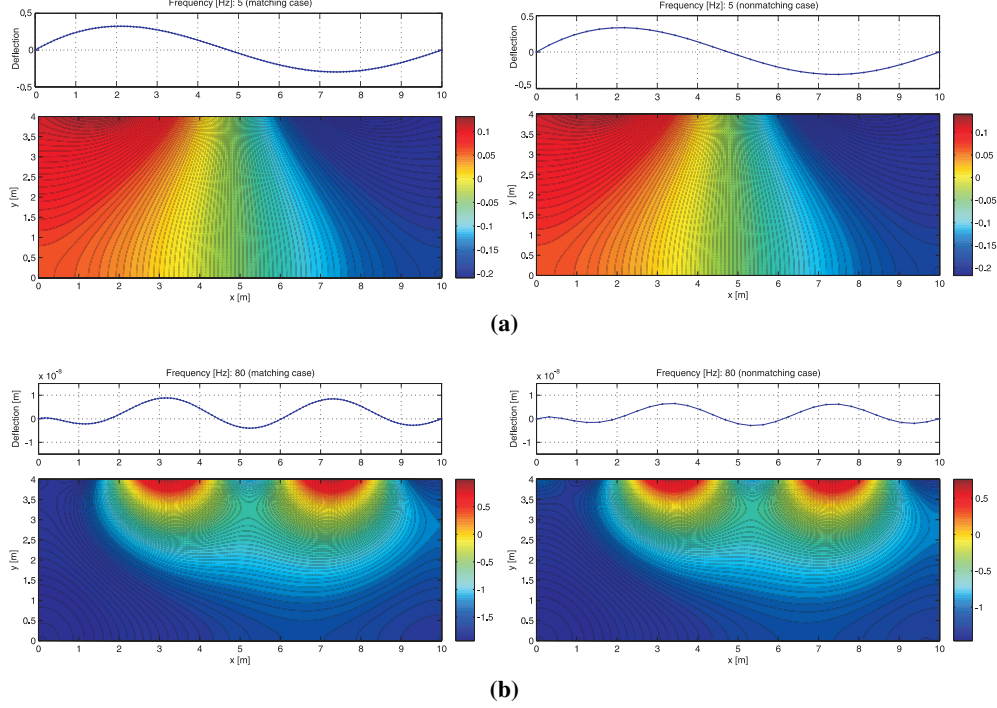


Figure 7: Acoustic cavity. Deflection of the flexible wall and fluid pressure field for different excitation frequencies. Results for 5 Hz (a) and 80 Hz (b) using matching meshes (left) and non-matching meshes (right).

The proposed preconditioners for the fluid and the structure are extensions of the well-known lumped and Dirichlet preconditioners of the standard FETI and AFETI algorithms. These preconditioners are calculated in a domain-by-domain basis as:

$$\tilde{\mathbf{F}}_{bb}^+ = \begin{cases} \bar{\mathbf{K}}_{bb} & \text{(FEM subdomain)} \\ \rho_F \omega^2 \mathbf{M}_{bb} \mathbf{H}_{bb}^{-1} \mathbf{G}_{bb} & \text{(BEM subdomain)} \end{cases} \quad (52)$$

where subscript (bb) refers to boundary extraction, i.e. pre and post multiplication by \mathbf{B}^\top and \mathbf{B} respectively.

Before an iterative method can be used to solve equation (42), a scaling of the variables based on [36] should be applied to improve the condition number of the system. Denoting $\Lambda = E\nu/((1+\nu)(1-2\nu))$, the scaled displacements are $\tilde{\mathbf{d}}_s = \sqrt{\rho\omega^2\Lambda} \mathbf{u}_S$ and $\tilde{\mathbf{d}}_f = \sqrt{\rho\omega^2\Lambda} \mathbf{u}_F$, and the scaled Lagrange multipliers $\tilde{\lambda} = 1/\sqrt{\rho\omega^2\Lambda} \lambda$.

5 Numerical Results

The possibilities of the proposed methodology are demonstrated in this section, where three representative examples are investigated solving the flexibility equation (47) using the nsBE-FETI iterative algorithm. The influence of different factors in the convergence of the nsBE-FETI algorithm like the number of elements per subdomain, frequency of the excitation and presence of non-matching interfaces, are examined.

5.1 Acoustic cavity with a flexible wall

This first example revisits the problem presented in section 3.3 (see Figure 5). A series of cases using BEM-FEM matching meshes are first solved. Fluid domain is discretized using linear boundary-element meshes with $L/h = 32, 64, 128, \text{ and } 256$ divisions at the interface and the structure is discretized using two-node Euler-Bernoulli beam elements. Two frequencies excitation of 5 Hz and 80 Hz are considered to study the influence of the frequency in the convergence.

Table 2 shows the number of iterations needed by the projected Bi-CGSTAB algorithm to solve these coupled problems with a tolerance of 10^{-10} . Figures 10(a) and 10(b) show the convergence evolution for a low excitation frequency of 5 Hz and a higher frequency of 80 Hz with the number of iterations needed by the algorithm to solve these problems. For the cases considered, it can be observed that an exponential increase of the type $L/h = 2^n$ translates into a constant

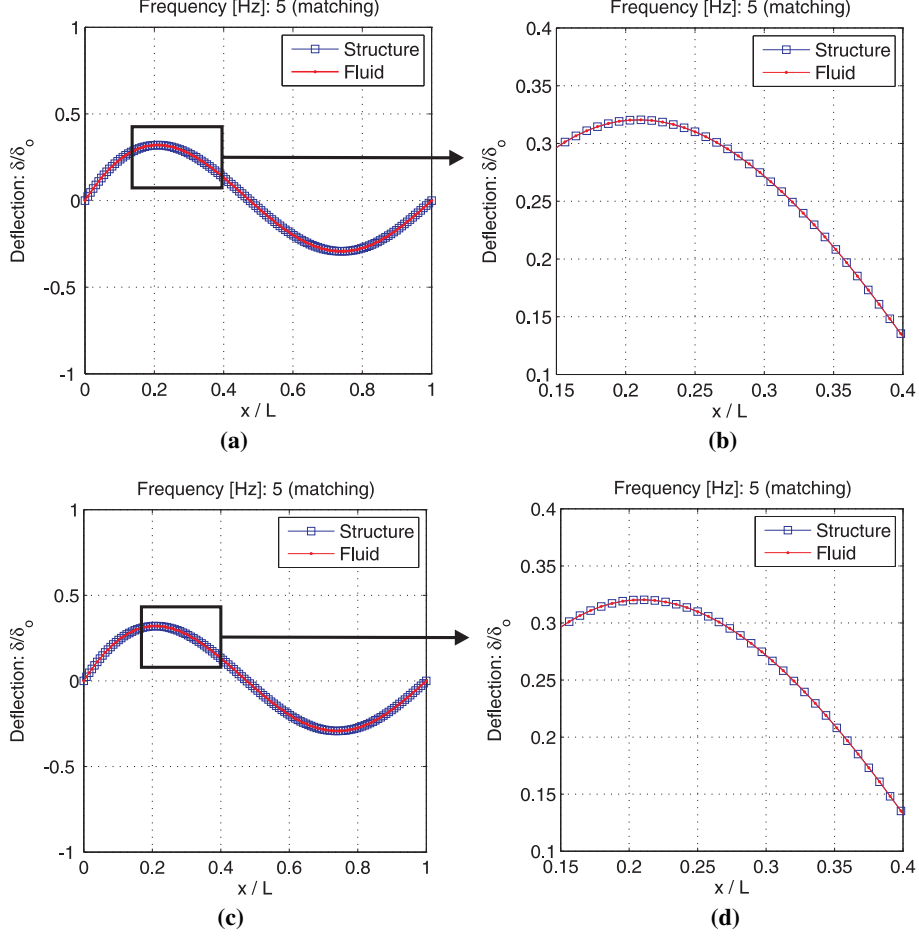


Figure 8: Beam deflection and interface fluid displacements for a bending moment with frequency $\omega = 5$ Hz. Interface coupling using matching meshes with mortar method (top) and LLM (bottom).

number of iterations for both excitation frequencies. The difference in the iterations number between 5 Hz and 80 Hz is due to the complexity of the solution, as Figure 11 shows.

Finally, the non-matching case is considered changing the discretization of the structure to produce dissimilar meshes at the interface. Figure 12 presents error evolutions for 5 Hz (Figure 12(a)) and 80 Hz (Figure 12(b)). The results are obtained for structural meshes ranging from $L/h = 64$ (highly non-matching case) to 256 (matching case) maintaining the mesh of the fluid fixed with $L/h = 256$ divisions. It is noted that the introduction of dissimilar meshes, maintaining a constant $(L/h)_{max}$, slightly increases the number-of-iterations needed by nsBE-FETI to solve the problem for low and high excitation frequencies. The experiment is repeated for the BEM-FEM case, see Table 3, presenting similar results. As a summary, in the matching case, the convergence of nsBE-FETI is governed by $(L/h)_{max}$, but the introduction of non-matching interfaces destructs this property producing a negative effect in the convergence that is controlled by the interface mesh-dissimilarity parameter h_{max}/h_{min} . However, for the cases studied, the impact of a non-matching interface is limited and does not significantly affect the algorithm convergence.

5.2 Rectangular duct with closed outlet

Next example considers a simple rectangular duct with a closed outlet as represented in Figure 13(a). The closed outlet is located at $x = L_o$ and assumed to be a rigid wall from $y = 0$ to $y = L$, and the inlet has a complex pressure ($p = p_o e^{i\omega t}$) prescribed at $x = 0$. The fluid is water as in the previous example. The wave number is set to $k = 1$, the length of the duct in the x -direction is $L_o = 8\pi m$ and the section height is $L = 1m$. Figure 13(b) presents the solution in terms of resulting pressure distribution on the field points.

(I) Initialize: $\lambda_0, \mathbf{r}_0 = \mathcal{P}(\mathbf{b} - \mathbf{F}_{bb}\lambda_0)$ $\mathbf{x}_0 = \mathbf{0}, \mathbf{p}_0 = \mathbf{0}$
(II) Iterate $i = 1, 2, 3, \dots$ until convergence: Compute: $\mathbf{p}_i = \mathbf{r}_{i-1} + \omega_i(\mathbf{p}_{i-1} - \alpha_{i-1}\mathbf{x}_{i-1})$ with $\mathbf{p}_1 = \mathbf{r}_0, \beta_i = (\hat{\mathbf{F}}_0^* \mathbf{r}_{i-1})$ and $\omega_i = \beta_i \gamma_{i-1} / (\alpha_{i-1} \beta_{i-1})$ Precondition: $\mathbf{a}_i = \tilde{\mathbf{F}}_{bb}^+ \mathbf{p}_i$ Projection: $\mathbf{z}_i = \mathcal{P} \mathbf{a}_i$ Compute: $\mathbf{u}_i = \mathbf{r}_{i-1} - \gamma_i \mathbf{x}_i,$ with $\mathbf{b}_i = \mathbf{F}_{bb} \mathbf{z}_i, \mathbf{x}_i = \mathcal{P} \mathbf{b}_i$ and $\gamma_i = \beta_i / (\hat{\mathbf{x}}_i^* \mathbf{r}_0)$ Precondition: $\mathbf{c}_i = \tilde{\mathbf{F}}_{bb}^+ \mathbf{u}_i$ Projection: $\mathbf{y}_i = \mathcal{P} \mathbf{c}_i$ Update solution: $\lambda_i = \lambda_{i-1} + \gamma_i \mathbf{z}_i + \alpha_i \mathbf{y}_i$ with $\mathbf{G}_i = \mathbf{F}_{bb} \mathbf{y}_i, \mathbf{w}_i = \mathcal{P} \mathbf{G}_i$ and $\alpha_i = (\hat{\mathbf{w}}_i^* \mathbf{u}_i) / (\hat{\mathbf{w}}_i^* \mathbf{w}_i)$ Update residual: $\mathbf{r}_i = \mathbf{u}_i - \alpha_i \mathbf{w}_i$
(III) If $\ \mathbf{r}_i\ / \ \mathbf{r}_0\ > \epsilon, i \leftarrow i + 1$ return to step (II)

Table 1: Complex BiCGStab algorithm with preconditioning and projection used to minimize the residual of equation (51).

L/h	n_e		Iterations	
	BEM	FEM	$5Hz$	$80Hz$
32	96	32	6	12
64	192	64	6	14
128	384	126	6	14
256	768	256	8	15

Table 2: Acoustic cavity problem with BEM-FEM matching interface. Number of iterations for a constant normalized residual with different mesh sizes.

L/h	L/h	Iterations	
		$5Hz$	$80Hz$
FEM	BEM		
64	256	8	15
128	256	18	25
256	256	20	30

Table 3: Acoustic cavity problem with BEM-FEM non-matching interface. Number of iterations for a normalized residual of 10^{-10} with different mesh sizes.

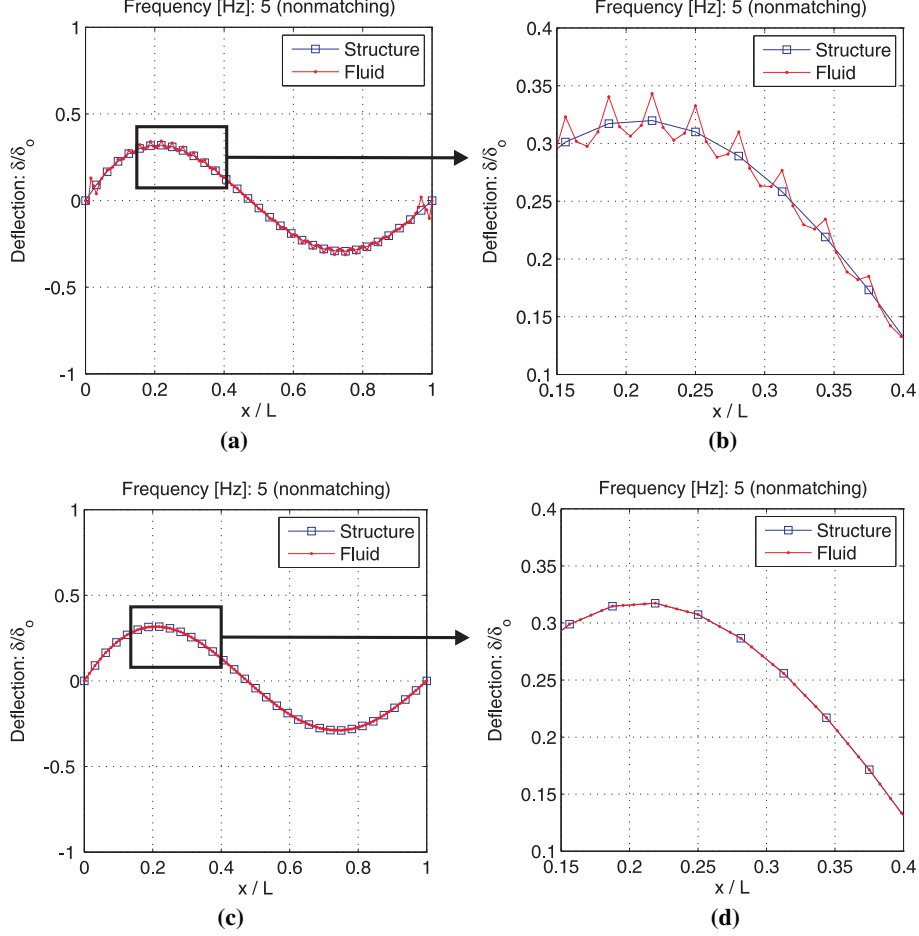


Figure 9: Beam deflection and interface fluid displacements for a bending moment of frequency $\omega = 5$ Hz. Interface coupling using non-matching meshes with mortar method (top) and LLM (bottom). In the mortar case, artifacts appear as a consequence of imposing the displacement compatibility condition in a weak sense (top-right).

L/h	n_p	n_e	Iterations
10	2	552	6
10	4	592	10
10	8	672	15

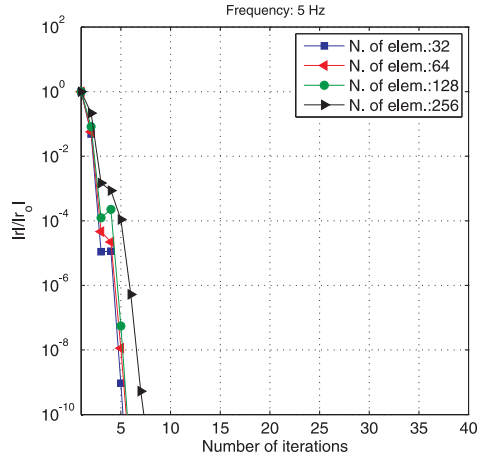
Table 4: Influence of the number of partitions (N_s) for a fixed mesh discretization (L/h) of the duct problem.

The duct is partitioned transversally into $N_s = 2, 4$ and 8 subdomains, discretized using linear boundary elements of fixed size $L/h = 10$, maintaining matching interfaces (Figure 14). The objective of this test is to demonstrate that, maintaining the element size, the convergence of nsBE-FETI is not considerably affected by the number of partitions. Table 4 contains a summary of convergence results, and Figure 15 shows the convergence history of this particular case. It is observed a small effect of N_s in the convergence.

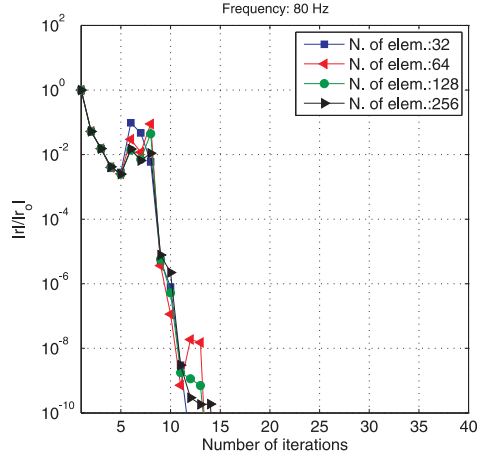
In the next experiment, the number of subdomains is fixed to $N_s = 4$ and the problem solved for different discretizations with $L/h = 10, 20$ and 40 , using a total of 148, 296 and 592 elements-per-subdomain. Convergence-rate results are summarized in Table 5, demonstrating a logarithmic correlation between the number of iterations for convergence and the mesh-size (L/h) in the range of discretization-sizes studied.

5.3 Open problem: Scattering object with a flexible wall

Finally, in our last example we consider an open problem with a square scattering object that has a flexible wall of length $L = 10$ m (Figure 16(a)). The fluid is water and the structural domain presents the same properties than the first



(a)



(b)

Figure 10: BiCGSTAB error evolution for: 5 Hz (a) and 80 Hz (b), considering a LLM coupling of matching meshes.

L/h	n_p	n_e	Iterations
10	4	592	10
20	4	1184	14
40	4	2368	18

Table 5: The number of partitions is fixed ($N_s = 4$) and the number of elements (N_{el}) increases.

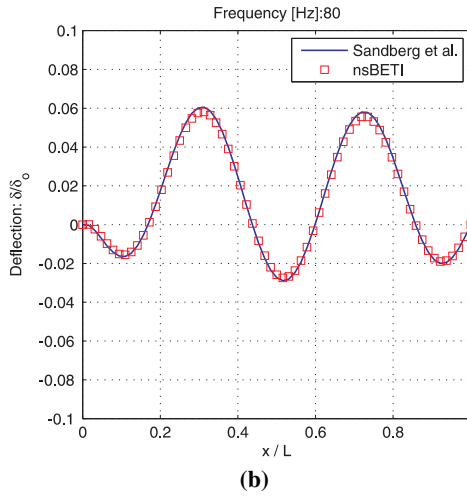
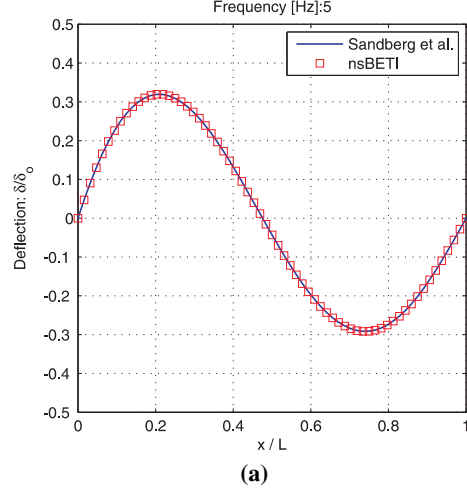


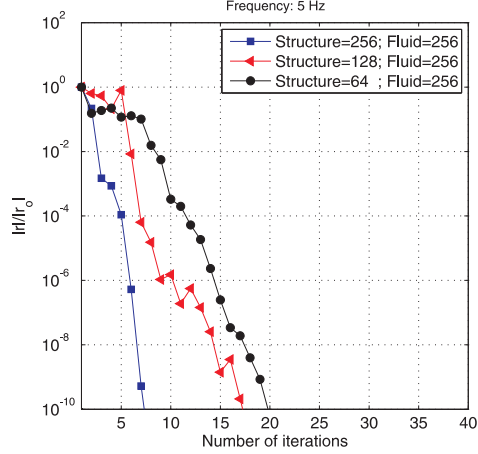
Figure 11: Beam deflection due to harmonic excitation of different frequencies: 5 Hz (a) and 80 Hz (b), considering a LLM coupling of matching meshes.

L/h	n_e BEM	n_e FEM	Iterations 500Hz
64	256	64	19
128	512	128	18
256	1024	256	18

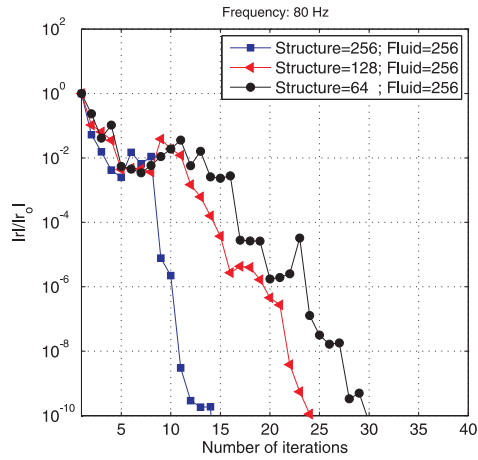
Table 6: Open problem with a BEM-FEM matching interface. Number of iterations for a constant normalized residual with different mesh sizes.

example. Our object is excited by a plane monochromatic wave of frequency 500 Hz and an incidence angle $\alpha = \pi/4$ rad.

The domains are discretized using the same number of elements at the coupling interface. Figure 16(b) shows the real part of the total acoustic pressure around the object. Table 6 presents the number of iterations needed by the projected Bi-CGSTAB algorithm to solve the coupled problem with a tolerance $\epsilon = 10^{-10}$ and Figure 17 shows the evolution of the residuals. It can be observed a similar behaviour of the algorithm in this exterior problem than in the interior cases previously studied.



(a)



(b)

Figure 12: Bi-CGSTAB error evolution considering non-matching meshes and harmonic excitations of: 5 Hz (a) and 80 Hz (b).

6 Summary and conclusions

NsBE-FETI, a FETI-type formulation, has been extended to treat non-matching and non-symmetrical BEM-FEM acoustic FSI problems. This new formulation enjoys similar scalability properties than the classical FETI and symmetrical-BETI algorithms.

This resolution scheme is based on the LLM methodology which allows to consider non-matching interfaces and preserves software modularity. A comparison between LLM and the mortar scheme reveals that the LLM method obtain a better interface displacements approximation than mortar for this kind of FSI problem: flexible wall discretized using cubic beam elements coupled with an acoustics fluid cavity, when highly dissimilar meshes are considered at the interfaces.

Some scalability properties of the nsBE-FETI scheme have been studied considering different physics. First example was an interior acoustic problem with a flexible wall, where fluid and structure were discretized using matching and non-matching meshes. It was found that, in the matching case, convergence of nsBE-FETI algorithm is governed by the element size $(L/h)_{max}$ but the introduction of non-matching interfaces produces a negative effect in the convergence that is controlled by the interface mesh-dissimilarity parameter h_{max}/h_{min} . However, for the cases studied, the impact of a non-matching interface is limited and does not significantly affect the algorithm convergence for low frequencies.

In the second example, we modify the number of subdomains. Convergence studies reveal that for a fixed element size, the nsBE-FETI is not considerably affected by the number of partitions (N_s). Furthermore, when the number of

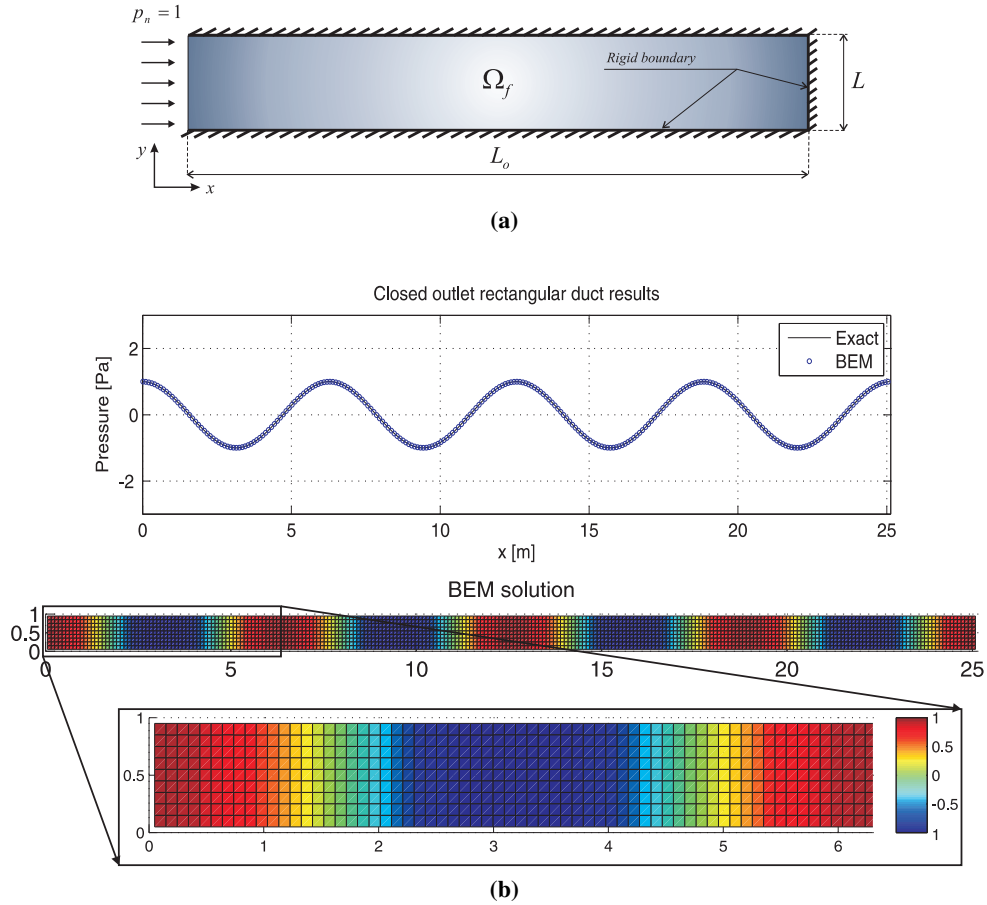


Figure 13: Rectangular duct with closed outlet. (a) Problem description, dimensions and boundary conditions. (b) Distribution of the fluid pressure in the longitudinal direction compared with the analytical solution.

subdomains is fixed and the problem solved for different discretizations, a logarithmic correlation between the number of iterations for convergence and the mesh-size used (L/h) is observed.

Finally, the last example presents an exterior FSI scattering problem where the same scalability behavior than in the interior ones could be observed. We can conclude that the proposed nsBE.FETI formulation equipped with the projected Bi-CGSTAB iterative solution algorithm presents good scalability properties for the solution of acoustic FSI problems.

7 Acknowledgements

This work was co-funded by the *Ministerio de Ciencia e Innovación* (Spain), through the research projects DPI2010-19331, which is co-funded with the European Regional Development Fund (ERDF) (*Fondo Europeo de Desarrollo Regional*, FEDER).

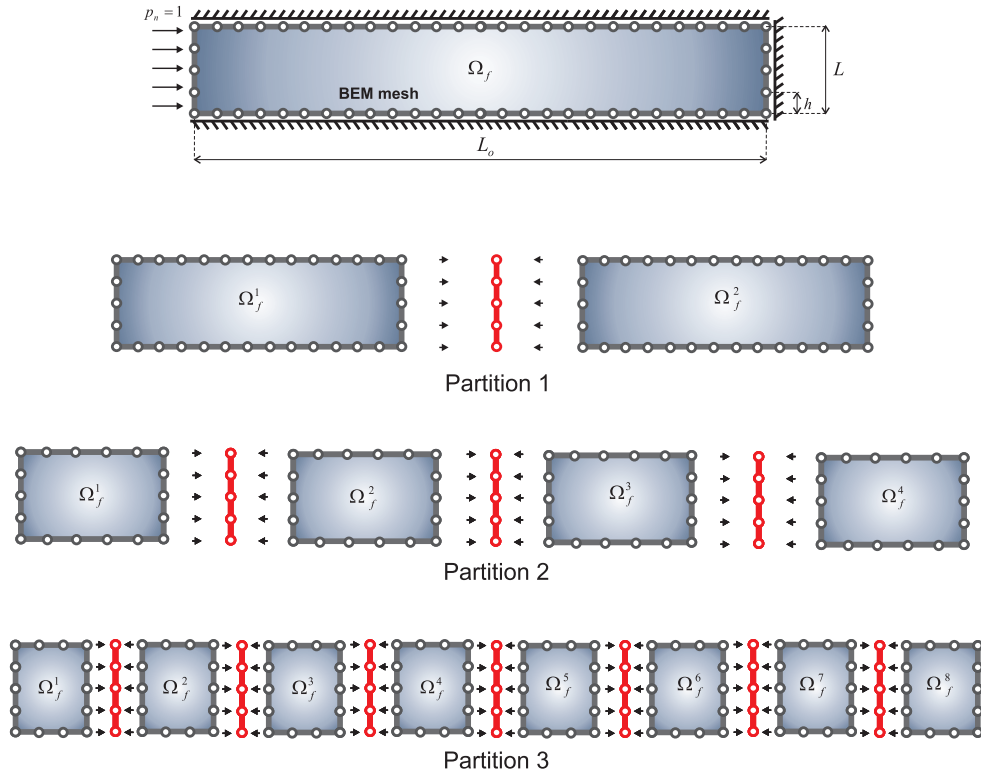


Figure 14: Rectangular duct with closed outlet. Partitioning of the fluid domain into $n_p=2, 4$ and 8 subdomains connected with localized Lagrange multipliers.

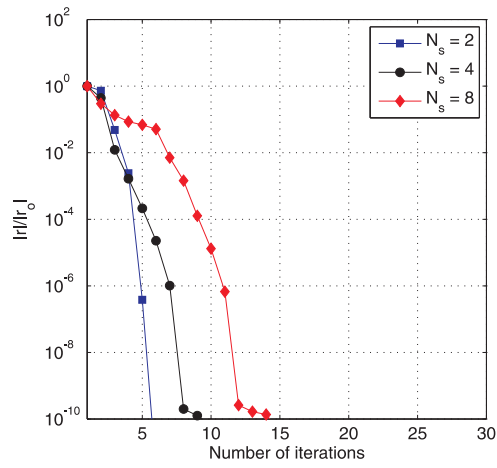


Figure 15: Duct problem. Evolution of the residual for different number of partitions.

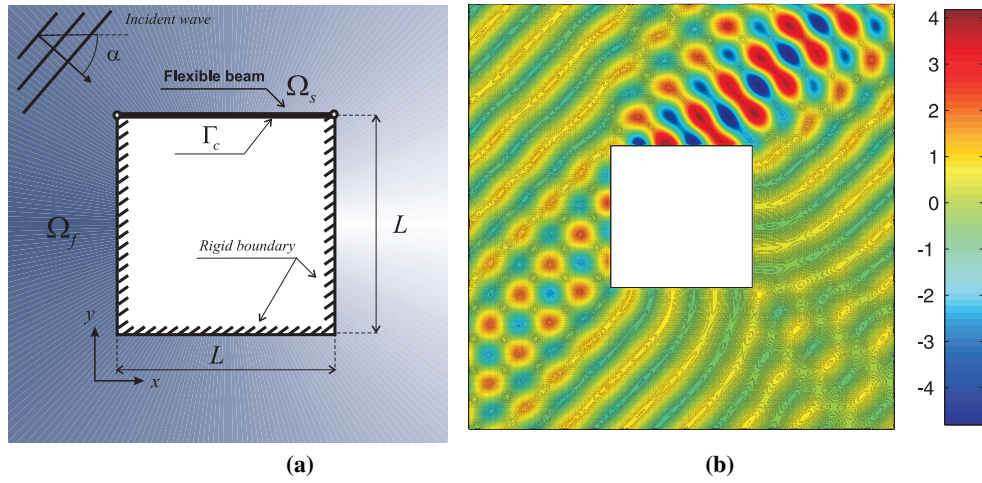


Figure 16: Wave scattering produced by a monochromatic incident wave on a square obstacle with a flexible wall. (a) Problem definition. (b) Real part of the total acoustic pressure for frequency 500 Hz and incidence angle $\alpha = -\pi/4$.

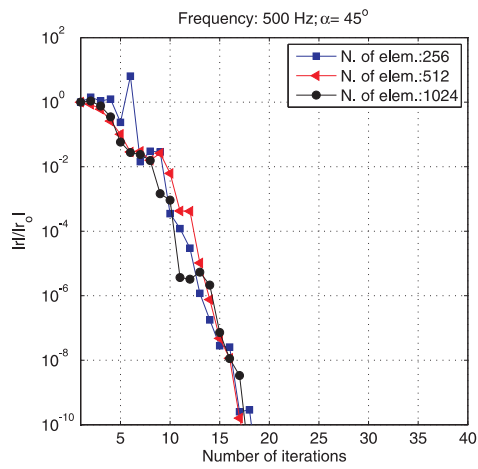


Figure 17: Scattering problem. Convergence of the projected Bi-CGSTAB algorithm for a frequency of 500 Hz with different meshes.

References

- [1] Morand, H., Ohayon, R. Fluid structure interaction: applied numerical interaction. John Wiley and Sons, 1995.
- [2] Ohayon, R., Soize, C., Structural acoustics and vibration. Academic Press: London, 1998.
- [3] Sandberg, G., Ohayon, R. Computational aspects of structural acoustics and vibration. Springer Wien New York, 2008.
- [4] Gaul, L., Kögl, M., Wagner, M., Boundary element method for engineers and scientists. Springer: Berlin, 2003.
- [5] Everstine, G.C., Henderson, F.M., Coupled finite element/boundary element approach for fluid structure interaction. *Journal of the Acoustical Society of America* 1990; **87**(5):1938-1947.
- [6] Chen, Z.S., Hofstetter, G., Mang, H.A., A Galerkin-type BE-FE formulation for elasto-acoustic coupling. *Comput. Meth. Appl. Mech. Eng.* 1998; **152**:147-155.
- [7] Gaul, L., Wenzel, W., A coupled symmetric BE-FE method for acoustic fluid-structure interaction. *Eng. Anal. Boundary Elem.* 2002; **26**(7):629-636.
- [8] Czygan, O., von Estorff, O., Fluid-structure interaction by coupling BEM and nonlinear FEM. *Engineering Analysis with Boundary Elements* 2002; **26**(9):773 -779.
- [9] Langer., S., Antes., H. Analysis of sound transmission through windows by coupled finite and boundary element methods. *Acta Acoustica* 2003; **89**:78-85.
- [10] Fritze, D., Marburg, S., Hardtke, H. FEM-BEM-coupling and structural-acoustic sensitivity analysis for shell geometries. *Comput. Struct.* 2005; **83**: 143–154.
- [11] Soares Jr., D. Fluid-structure analysis by optimised boundary element-finite element coupling procedures. *J. Sound Vib.* 2009; **322**: 184–195.
- [12] He., Z.C., Liu., G.R., Zhong, Z.H., Zhang, G.Y., Cheng, A.G. A coupled Es-FEM/BEM method for fluid-structure interaction problems. *Eng. Anal. Boundary Elem.* 2011; **35**:140-147.
- [13] Soares Jr., D., Godinho, L. An optimized BEM-FEM iterative coupling algorithm for acoustic-elastodynamic interaction analyses in the frequency domain. *Comput. Struct.* 2012; **106-107**: 68–80.
- [14] Fischer, M., Gaul, L. Fast BEM-FEM mortar coupling for acoustics-structure interaction. *Int. J. Numer. Methods Eng.* 2005; **62**: 1677–1690.
- [15] Bernardi, C. and Maday, Y. and Patera, A new nonconforming approach to domain decomposition: the mortar element method. In: H. Brezis and J. L. Lions (Eds.), *Non linear partial differential equations and their applications*. Pitman and Wiley, New York, 1994; 13-51.
- [16] K.C. Park, C.A. Felippa: A variational principle for solution method developments in structural mechanics. *Journal of Applied Mechanics*, 65 (1998), 242-249.
- [17] K.C. Park, C.A. Felippa: A variational principle for the formulation of partitioned structural systems. *Int. J. Num. Meth. Engng.*, 47 (2000), 395-418.
- [18] K.C. Park, C.A. Felippa, G. Rebel: A simple algorithm for localized construction of non-matching structural interfaces. *Int. J. Num. Meth. Engng.*, 53 (2002), 2117-2142.
- [19] González, J.A., Park, K.C. BEM and FEM coupling in elastostatics using localized Lagrange multipliers. *Int. J. Numer. Methods Eng.* 2007; **69**: 2058-2074.
- [20] Park, K.C., Felippa, C.A., Ohayon, R. Partitioned formulation of internal fluid-structure interaction problems by localized Lagrange multipliers. *Comput. Meth. Appl. Mech. Eng.* 2001; **190**: 2989-3007.
- [21] Ross, M.R., Felippa, C.A., Park, K.C., Sprague, M.A. Treatment of acoustic fluid-structure interaction by localized Lagrange multipliers: Formulation. *Comput. Meth. Appl. Mech. Eng.* 2008; **197**: 3057-3079.
- [22] Ross, M.R., Sprague, M.A., Felippa, C.A., Park, K.C. Treatment of acoustic fluid-structure interaction by localized Lagrange multipliers and comparison to alternative interface-coupling methods. *Comput. Meth. Appl. Mech. Eng.* 2009; **198**: 986-1005.
- [23] Park, K.C., Ohayon, R., Felippa, C.A., González, J.A. Partitioned formulation of internal and gravity waves interacting with flexible structures. *Comput. Meth. Appl. Mech. Eng.* 2010; **199**: 723-733.
- [24] González, J.A., Park, K.C. A simple explicit-implicit finite element tearing and interconnecting transient analysis algorithm. *Int. J. Numer. Methods Eng.* 2012; **89**: 1203-1226.
- [25] González, J.A., Park, K.C., Lee, I., Felippa, C.A., Ohayon, R. Partitioned vibration analysis of internal fluid-structure interaction problems. *Int. J. Numer. Methods Eng.* 2012; **92**: 268-300.

- [26] C. Farhat, F. Roux: A method of finite element tearing and interconnecting and its parallel solution algorithm. *International Journal for Numerical Methods in Engineering*, 32 (1991), 1205-1227.
- [27] M. Bhardwaj, D. Day, C. Farhat: Application of the FETI method to ASCI problems-scalability results on 1000 processors and discussion of highly heterogeneous problems. *International Journal for Numerical Methods in Engineering*, 47 (2000), 513-535.
- [28] C. Farhat, K. Pierson, M. Lesoinne: The second generation FETI methods and their application to the parallel solution of large-scale linear and geometrically non-linear structural analysis problems. *Computer Methods in Applied Mechanics and Engineering*, 184 (2000), 333-374.
- [29] C. Farhat, J. Mandel: The two-level FETI method for static and dynamic plate problems Part I: An optimal iterative solver for biharmonic systems. *Computer Methods in Applied Mechanics and Engineering*, 155 (1998), 129-151.
- [30] C. Farhat, P. Chen, J. Mandel, F. Roux: The two-level FETI method Part II: Extension to shell problems, parallel implementation and performance results. *Computer Methods in Applied Mechanics and Engineering*, 155 (1998), 153-179.
- [31] J. Mandel, R. Tezaur: Convergence of a substructuring method with Lagrange multipliers. *Numerische Mathematik*, 73 (1996), 473-487.
- [32] C. Farhat, M. Lesoinne, K. Pierson: A scalable dual-primal domain decomposition method. *Numerical Linear Algebra with Applications*, 7 (2000), 687-714.
- [33] C. Farhat, M. Lesoinne, P. LeTallec, K. Pierson, D. Rixen: FETI-DP: a dual-primal unified FETI method -part I: A faster alternative to the two-level FETI method. *International Journal for Numerical Methods in Engineering*, 50 (2001), 1523-1544.
- [34] Farhat, C., Macedo, A., Lesoinne, M. A two-level domain decomposition method for the iterative solution of high frequency exterior Helmholtz problems. *Numerische Mathematik* 2000; **85**: 283-308.
- [35] Farhat, C., Macedo, A., Lesoinne, M., Roux, F., Magnoulès, F., de La Bourdonnaie, A. Two-level domain decomposition methods with Lagrange multipliers for the fast iterative solution of acoustic scattering problems. *Comput. Meth. Appl. Mech. Eng.* 2000; **184**: 213-239.
- [36] Li, J., Farhat, C., Avery, P., Tezaur, R. A dual-primal FETI method for solving a class of fluid-structure interaction problems in the frequency domain. *Int. J. Numer. Methods Eng.* 2012; **89**: 418-437.
- [37] U. Langer, O. Steinbach: Boundary element tearing and interconnecting methods. *Computing*, 71 (2003), 205-228.
- [38] M. Bonnet, G. Maier, C. Polizzotto: Symmetric Galerkin boundary element method. *ASME Appl. Mech. Rev.*, 51 (1998), 669-704.
- [39] L.J. Gray, G.H. Paulino: Symmetric galerkin boundary integral formulation for interface and multi-zone problems. *International Journal for Numerical Methods in Engineering*, 40 (1997), 3085-3101.
- [40] G. Of, O. Steinbach: The all-floating boundary element tearing and interconnecting method. *J. Num. Math.*, 17 (2009), 277-298.
- [41] J. Bouchala, Z. Dostál, M. Sadowská: Scalable total BETI based algorithm for 3D coercive contact problems of linear elastostatics. *Computing*, 85 (2009), 189-217.
- [42] K.C. Park, M.J. Filho, C.A. Felippa: An algebraically partitioned FETI method for parallel structural analysis: algorithm description. *International Journal for Numerical Methods in Engineering*, 40 (1997), 2717-2737.
- [43] M.J. Filho, K.C. Park, C.A. Felippa: An algebraically partitioned FETI method for parallel structural analysis: performance evaluation. *International Journal for Numerical Methods in Engineering*, 40 (1997), 2739-2758.
- [44] González, J.A., Rodríguez-Tembleque, L., Park, K.C., Abascal, R. The nsBETI method: an extension of the FETI method to non-symmetrical BEM-FEM coupled problems. *Int. J. Numer. Methods Eng.* 2013; **93**: 1015–1039.
- [45] Wu, T.W. Boundary element in acoustics: fundamentals and computer codes. WIT Press, Southampton, 2000.
- [46] Bonnet, M. Encyclopedia of Computational Mechanics: Boundary integral equation methods for elastic and plastic methods, volume 2. John Wiley and Sons, 2004.
- [47] Sandberg, G., Wernberg, P., Davidson, P. Fundamentals of fluid-structure interaction. In: G. Sandberg and R. Ohayon (Eds.), Computational aspects of structural acoustics and vibration. Springer Wien New York, 2008; 23-102.
- [48] Wohlmuth, B. I. A mortar finite element method using dual spaces for the Lagrange multiplier. *SIAM Journal on Numerical Analysis*, **38**, (2000), 989–1012, 2000.